

Electron-optical phonon scattering in doped GaAs quantum well

V. Ya. Aleshkin^{*} and A. A. Dubinov[†]

Department of Semiconductor Physics, Institute for Physics of Microstructures RAS, Nizhny Novgorod 603950, Russia and Lobachevsky State University of Nizhny Novgorod, Nizhny Novgorod 603950, Russia

 (Received 21 March 2024; revised 30 May 2024; accepted 1 July 2024; published 15 July 2024)

The influence of the presence of free electrons on the spectra of optical phonons and on electron-optical phonon scattering in quantum wells has been theoretically studied. As an example, calculations of the optical phonon spectra, intrasubband and intersubband electron-optical phonon scattering in 10-nm-GaAs quantum wells surrounded by $\text{Al}_{0.3}\text{Ga}_{0.7}\text{As}$ barriers were carried out at two temperatures of 77 and 300 K. It was shown that the frequency of intrasubband scattering varies nonmonotonically with increasing electron concentration in the quantum well. The relaxation rates of the wave vector and energy for scattering in the first and second subbands are found. It is shown that with increasing electron concentration in the quantum well, the frequency of intersubband scattering decreases.

DOI: [10.1103/PhysRevMaterials.8.074602](https://doi.org/10.1103/PhysRevMaterials.8.074602)

I. INTRODUCTION

Electron-optical phonon scattering is one of the main mechanisms of electron energy relaxation in semiconductors. It plays an important role in the operation of many semiconductor devices, including devices that use quantum wells. Examples of such devices include injection lasers with quantum wells (QWs) [1], quantum cascade lasers (QCLs) [2,3], and quantum well radiation detectors (QWIPs) [4]. These processes are especially important in QCLs, in which the populations of working levels are often determined by the scattering of electrons by optical phonons [3].

It is well known that the optical phonon properties in quantum wells differ from those in bulk semiconductors. This was pointed out in Ref. [5], in which optical phonons in a slab of a polar semiconductor with an isotropic dielectric permittivity were studied. It was shown that the optical phonons in such a system can be divided into two groups: bulklike and surface [5,6]. For bulklike optical phonons, lattice vibrations are concentrated inside the slab (quantum well) and are absent outside it. For surface optical phonons, lattice vibrations are concentrated near the slab boundaries. In Refs. [7,8], the optical phonons were considered in quantum wells with a wurtzite structure, where the dielectric permittivity is anisotropic. In a number of works [7–16], the rates of electron-optical phonon scattering in quantum wells in which there are no free carriers were calculated.

It is interesting to note that until recently the influence of electrons in a quantum well on the properties of the optical phonons in it was not considered. The physical reason for this effect is that both optical lattice vibrations and electron density oscillations create an electric field. This field affects both lattice vibrations and electron density oscillations. Or,

in other words, the contribution of electrons to the dielectric constant of a quantum well changes the properties of the optical phonons in it.

To date, two approaches have been outlined to take into account the influence of electrons in a quantum well on the properties of the optical phonons in it. In the first approach, the influence of free carriers was taken into account only as static screening of the electric potential, i.e., in electronic polarizability, its dependence on frequency was not taken into account [17–19]. This approach has been used to study phonons in graphene [17] and GaSe [18] and InSe [19] layers that include several atomic planes. As noted in Ref. [17], this approximation ignores plasmonic effects.

The second approach is to take into account plasmonic effects in electronic polarization [20–22]. In Ref. [20], electron scattering by optical phonons in MoS_2 monolayers was considered. Note that in Refs. [17–20] systems were considered in which the thickness of quantum wells is much smaller than the characteristic scale of the change of the electric field created by the phonon. Therefore, in these works, the change in the electric potential inside the quantum well was neglected. In this work, as in Refs. [21,22], the width of the quantum well is on the order of the scale of the change of the phonon electric field. For this reason, when calculating the phonon spectrum and electron-phonon scattering rates, it is necessary to take into account the change of the electric field of phonons inside the QW.

A significant change in the spectra of optical phonons in quantum wells of narrow-gap $\text{HgTe}/\text{CdHgTe}$ heterostructures due to plasmonic effects was shown in Refs. [21,22]. However, these works did not take into account the spatial dispersion of electronic polarizability, which must be taken into account for a correct description of the phonon spectrum at sufficiently large vectors ($q \geq \omega/v$), where ω is the phonon frequency, v is the characteristic electron velocity. The energy of a longitudinal optical phonon in GaAs approximately equals 36 meV, and the electron effective mass

^{*}Contact author: aleshkin@ipmras.ru

[†]Contact author: sanya@ipmras.ru

is $0.067 m_0$ where m_0 is a free electron mass. The thermal speed of an electron at a temperature of 300 K in a quantum well is about $3 \cdot 10^7$ cm/s. Therefore, wave vectors at which the spatial dispersion of the electronic contribution to the dielectric permittivity is significant must satisfy the condition $q \geq 0.15 \text{ nm}^{-1}$. If we take the wave vector of an electron, whose energy is equal to the optical phonon energy, as the characteristic vector of the optical phonon involved in scattering, then we obtain the value $q = 0.25 \text{ nm}^{-1}$. From the above estimates, it is obvious that taking into account the spatial dispersion of the electronic contribution to the dielectric permittivity of the QW is important for calculating electron-optical phonon scattering in GaAs QWs.

The purpose of this work is to develop the approach proposed in Refs. [21,22], by taking into account the spatial dispersion of the contribution to the dielectric permittivity of the quantum well from electrons located in the QW. In this work, using the example of a 10-nm GaAs QW surrounded by $\text{Al}_{0.3}\text{Ga}_{0.7}\text{As}$ barriers, we studied the effect of the concentration of electrons located in the conduction band of the QW on the optical phonon spectra and on the probabilities of electron-optical phonon scattering. Note that the use of QWs with a high electron concentration ($>10^{11} \text{ cm}^{-3}$) can significantly reduce the number of cascades required to implement terahertz QCLs [23].

II. OPTICAL PHONONS IN A DOPED GaAs/AlGaAs HETEROSTRUCTURE

To describe the optical phonon spectrum, we will use the dielectric continuum model developed for semiconductors with an isotropic dielectric constant in Refs. [5,6], and for semiconductors with an anisotropic dielectric constant in Refs. [7,8]. This model works well when the QW width is much larger than the lattice constant.

Recall that in the dielectric continuum model, the medium is characterized by a local dielectric permittivity. However, it is known that the dielectric permittivity of a two-dimensional electron gas κ is nonlocal [24] and the relationship between the electric induction D and the electric field E has the form

$$D(z) = \frac{1}{d} \int dz' \kappa(z, z') E(z'), \quad (1)$$

where d is the QW width and the direction z is chosen along the normal to the QW. To avoid computational difficulties caused by the nonlocality of the dielectric permittivity, we use the following approximation. If we assume the scale of the change of the electric field along the z direction is much greater than the QW width, then Eq. (1) can be rewritten as

$$D(z) \approx E(z) \frac{1}{d} \int dz' \kappa(z, z'). \quad (2)$$

In this case, the dielectric permittivity of the electron gas is characterized by an ‘‘averaged’’ local value: $\kappa(z) = d^{-1} \int dz' \kappa(z, z')$. In the problem under consideration, the scale of change in the field E is of the order of the QW width, and this approximation reduces the accuracy of the results obtained.

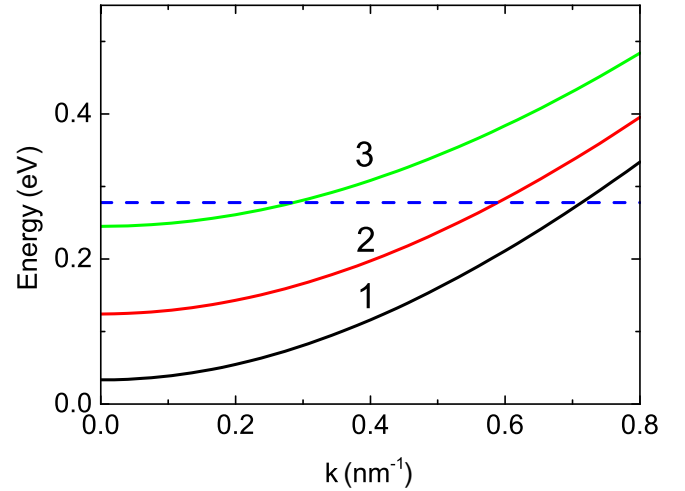


FIG. 1. Electron spectrum in a 10-nm GaAs quantum well. The dotted line corresponds to the bottom of the $\text{Al}_{0.3}\text{Ga}_{0.7}\text{As}$ conduction band. The energy reference point corresponds to the bottom of the GaAs conduction band. The numbers in the figure indicate the subband numbers.

Let us consider a 10-nm GaAs quantum well surrounded by $\text{Al}_{0.3}\text{Ga}_{0.7}\text{As}$ barriers. This quantum well thickness and barrier composition are typical for interband diode lasers in the 808–850-nm range [25–27], as well as THz QCLs with operating temperatures above 200 K [28–30]. We will assume that the structure is grown on the (001) plane. For simplicity, we will assume the QW is rectangular, i.e., we neglect the influence of electrons on its shape.

Figure 1 shows the electron spectrum in the QW under consideration, calculated in the Kane model taking into account deformation effects. The explicit form of the Kane Hamiltonian and details of the calculations are given in [31]. It can be seen from Fig. 1 that in the conduction band of the quantum well there are three size quantization subbands. The distance between the first and second subbands is 91 meV and between the first and third subbands is 212 meV. Calculations show that in such a quantum well at electron concentrations of no more than 10^{12} cm^{-2} and temperatures at room temperature and below, the main part of the electron is located in the first and second subbands. The contribution to the dielectric permittivity from a two-dimensional electron gas in the frequency range corresponding to the optical phonons is determined by two types of electron motion. The first type of movement is intrasubband. The second type of motion is intersubband, as a result of which an electron transits from one subband to another. The conductivity of electrons along a quantum well in the system under consideration is determined by intrasubband motion, and across the quantum well by intersubband electronic transitions. Since the electronic conductivities along and across the quantum well are different, the contribution to the dielectric permittivity from free electrons is a tensor.

Intrasubband electron motion contributes only to the diagonal components of the dielectric permittivity in the QW plane, since this motion occurs along the QW (for an electron with a quadratic dispersion law). The contribution to the dielectric permittivity of intrasubband electron motion within the random phase approximation (RPA) framework can be

represented as

$$\begin{aligned}\kappa_{xx}^{\text{intra}}(\mathbf{q}, \omega) &= \kappa_{yy}^{\text{intra}}(\mathbf{q}, \omega) \\ &= \frac{4\pi e^2}{Sd q^2} \sum_{\mathbf{k}, j} \frac{f_j(\mathbf{k}) - f_j(\mathbf{k} + \mathbf{q})}{\varepsilon_j(\mathbf{k}) - \varepsilon_j(\mathbf{k} + \mathbf{q}) + \hbar\omega + i\hbar\alpha},\end{aligned}\quad (3)$$

where \mathbf{q} and ω are the wave vector and cyclic frequency of the wave propagating along the QW, respectively, S is the QW square, e is the electron charge, index j includes the subband number and spin index, $\varepsilon_j(\mathbf{k})$ is the energy of the electron in the j th state with the wave vector \mathbf{k} , $f_j(\mathbf{k})$ is the electron distribution function, α is an infinitesimal positive quantity, \hbar is Planck's constant. Further we will assume that $f_j(\mathbf{k})$ is the Fermi-Dirac distribution function.

Since electrons occupy a small part of the space of wave vectors, to simplify the calculation of (3) we will assume that the electron mass is isotropic and independent of the electron energy. In this case, the sum over the wave vector in Eq. (3) is reduced to a one-dimensional integral (see Appendix A).

Intersubband electron transitions contribute only to the zz component of the dielectric permittivity tensor:

$$\kappa_{zz}^{\text{inter}}(\mathbf{q}, \omega) = \frac{4\pi e^2}{dS} \sum_{l, m, \mathbf{k}} \frac{|z_{\mathbf{k}+\mathbf{q}, m; \mathbf{k}, l}|^2 [f_l(\mathbf{k}) - f_m(\mathbf{k} + \mathbf{q})]}{\varepsilon_m(\mathbf{k} + \mathbf{q}) - \varepsilon_l(\mathbf{k}) - \hbar\omega - i\hbar\alpha},\quad (4)$$

where $z_{\mathbf{k}+\mathbf{q}, m; \mathbf{k}, l}$ is the matrix element of the operator \hat{z} between the state of the electron located with the wave vector $\mathbf{k} + \mathbf{q}$ in the m th subband and the state of the electron with the wave vector \mathbf{k} in the l th subband. The derivation of Eq. (4) is given in Appendix B. To simplify the calculation of (4), we will assume the electron masses in the first and second subbands to be the same. In this case, the sum over the wave vector in (4) is also reduced to a one-dimensional integral (see Appendix B). Note that the calculation in the Kane model shows the difference in electron masses by no more than 5% in the range of wave vectors (0–0.6 nm⁻¹). In addition, the effective masses at the bottom of the first and second size quantization subbands differ by 13%. Therefore, the assumption made about the constancy of the electron mass is a reasonable approximation.

The diagonal components of the dielectric permittivity tensor can be written as

$$\kappa_{jj}(\mathbf{q}, \omega) = \delta_{j,j} \kappa^{\text{latt}}(\omega) + \kappa_{jj}^{\text{intra}}(\mathbf{q}, \omega) + \kappa_{jj}^{\text{inter}}(\mathbf{q}, \omega),\quad (5)$$

where $\kappa^{\text{latt}}(\omega)$ is the dielectric permittivity of a quantum well without electrons, which in the frequency range under consideration can be represented as [32]

$$\kappa^{\text{latt}}(\omega) = \kappa_{\infty} \frac{\omega^2 - \omega_L^2}{\omega^2 - \omega_T^2},\quad (6)$$

where κ_{∞} is the high-frequency dielectric constant of the quantum well material and ω_L and ω_T are the longitudinal and transverse optical phonon frequencies in the QW, respectively.

The barrier is a ternary solid solution. Let us assume that there are no electrons in it. Then the barrier dielectric

permittivity can be written in the following form [15]:

$$\kappa_b(\omega) = \kappa_{\infty b} \frac{(\omega^2 - \omega_{\text{LGaAs}}^2)(\omega^2 - \omega_{\text{LAiAs}}^2)}{(\omega^2 - \omega_{\text{TGaAs}}^2)(\omega^2 - \omega_{\text{TAiAs}}^2)},\quad (7)$$

where $\kappa_{\infty b}$ is the high-frequency dielectric constant of the barrier, ω_{LGaAs} and ω_{TGaAs} are the frequencies of longitudinal and transverse GaAs-like optical phonons, and ω_{LAiAs} and ω_{TAiAs} are the frequencies of longitudinal and transverse AlAs-like optical phonons. For calculations, the quantities ω_L , ω_T , ω_{LGaAs} , ω_{TGaAs} , ω_{LAiAs} , ω_{TAiAs} , κ_{∞} , and $\kappa_{\infty b}$ were taken from Ref. [33].

The phase velocities of the optical phonons taking part in electron scattering are much lower than the speed of light. Therefore, the electric fields created by lattice vibrations and electron density oscillations can be described using an electric potential. Let the phonon propagate along the x direction. Then the electric potential $\varphi_q(\mathbf{r}, t)$ created by the optical phonon with wave vector q can be represented in the following form:

$$\varphi_q(\mathbf{r}, t) = [c_q \exp(iqx - i\omega t) + \text{c.c.}] \Phi_q(z, \omega),\quad (8)$$

where c_q are the coefficients that determine the potential value and the symbol c.c. stands for the complex conjugate term, and $\Phi_q(z, \omega)$ is a dimensionless function describing the dependence of potential on z and ω .

For a medium with an anisotropic dielectric permittivity depending on the z coordinate, Maxwell's equation for electrical induction can be written in the form [7,8]

$$-q^2 \kappa_{xx}(q, \omega, z) \Phi_q(z, \omega) + \frac{\partial}{\partial z} \left(\kappa_{zz}(q, \omega, z) \frac{\partial \Phi_q(z, \omega)}{\partial z} \right) = 0.\quad (9)$$

Let the quantum well occupy the region $|z| < d/2$. The system under consideration has a plane of symmetry at $z = 0$. Therefore, solutions to Eq. (9) can be divided into even and odd ones. For even solutions, the dependence $\Phi_q(z, \omega)$ on z has the form [21]

$$\Phi_q(z, \omega) = \begin{cases} \cos(\beta_q(\omega)qz), & |z| < d/2, \\ \cos\left(\frac{\beta_q(\omega)qd}{2}\right) \exp\left(\frac{qd}{2} - q|z|\right), & |z| > \frac{d}{2}, \end{cases}\quad (10)$$

where $\beta_q(\omega) = \sqrt{-\kappa_{xx}(q, \omega)/\kappa_{zz}(q, \omega)}$. Expression (10) is valid in the frequency range where $\kappa_{xx}(q, \omega)\kappa_{zz}(q, \omega) < 0$. In the frequency range where $\kappa_{xx}(q, \omega)\kappa_{zz}(q, \omega) > 0$, solution (9) can be represented as

$$\Phi_q(z, \omega) = \begin{cases} \cosh(\gamma_q(\omega)qz), & |z| < d/2, \\ \cosh\left(\frac{\gamma_q(\omega)qd}{2}\right) \exp\left(\frac{qd}{2} - q|z|\right), & |z| > \frac{d}{2}, \end{cases}\quad (11)$$

where $\gamma_q(\omega) = \sqrt{\kappa_{xx}(q, \omega)/\kappa_{zz}(q, \omega)}$. Similarly, we can write odd solutions in the frequency range where the condition $\kappa_{xx}(q, \omega)\kappa_{zz}(q, \omega) < 0$ is satisfied:

$$\Phi_q(z, \omega) = \begin{cases} \sin(\beta_q(\omega)qz), & |z| < d/2, \\ \frac{z}{|z|} \sin\left(\frac{\beta_q(\omega)qd}{2}\right) \exp\left(\frac{qd}{2} - q|z|\right), & |z| > \frac{d}{2}, \end{cases}\quad (12)$$

and in the frequency range where the inequality $\kappa_{xx}(q, \omega)\kappa_{zz}(q, \omega) > 0$ is true:

$$\Phi_q(z, \omega) = \begin{cases} \sinh(\gamma_q(\omega)qz), & |z| < d/2, \\ \frac{z}{|z|} \sinh\left(\frac{\gamma_q(\omega)qd}{2}\right) \exp\left(\frac{qd}{2} - q|z|\right), & |z| > \frac{d}{2}, \end{cases} \quad (13)$$

When $\kappa_{xx}(q, \omega) \rightarrow \kappa_{zz}(q, \omega)$, solutions (10) and (12) transform into known solutions for bulklike phonons [5,6], and (11) and (13) into solutions for surface phonons. Therefore, we will further call phonons corresponding to solutions (10) and (12) bulklike ones, and phonons corresponding to solutions (11) and (13) surface ones.

Functions (10)–(13) are continuous at the boundaries of the QW. From the condition for matching the derivative, we obtain equations for determining the spectrum of optical phonons. For even bulklike phonons, this equation is given in Eq. (14), and for surface phonons in Eq. (15) [21]:

$$\kappa_{zz}(q, \omega)\beta_q(\omega) \tan(\beta_q(\omega)qd/2) = \kappa_b(\omega), \quad (14)$$

$$\kappa_{zz}(q, \omega)\gamma_q(\omega) \tanh(\gamma_q(\omega)qd/2) = -\kappa_b(\omega). \quad (15)$$

Similar equations for odd bulklike phonons are given in Eq. (16), and for surface phonons in Eq. (17):

$$\kappa_b(\omega) \tan[\beta_q(\omega)qd/2] = -\kappa_{zz}(q, \omega)\beta_q(\omega), \quad (16)$$

$$\kappa_b(\omega) \tanh[\gamma_q(\omega)qd/2] = -\kappa_{zz}(q, \omega)\gamma_q(\omega). \quad (17)$$

Figure 2 shows the calculated spectra of even phonons for the structure under consideration for four electron concentrations in the QW ($0, 10^{11}, 3 \times 10^{11}$ and 10^{12} cm^{-2}) and two temperatures (77 and 300 K). The quantum well contains four optical phonons with energies of $\sim 46, 36, 35,$ and 33 meV . In the absence of electrons in the QW, all branches except the branch with an energy close to the energy of the longitudinal optical phonon in GaAs ($\sim 36 \text{ meV}$) are surface ones. This statement remains valid for electron concentrations of $10^{11}, 3 \times 10^{11} \text{ cm}^{-2}$. At a concentration of $n = 10^{12} \text{ cm}^{-2}$, the high-frequency branch at $0 < q < 0.12 \text{ nm}^{-1}$ at 300 K and at $0 < q < 0.16 \text{ nm}^{-1}$ at $T = 77 \text{ K}$ is bulklike, and outside this interval it is a surface one.

It can be seen from the Fig. 2 that an increase in the electron concentration most strongly affects the two high-frequency phonon branches in the region of wave vectors $q < 1 \text{ nm}^{-1}$. This influence increases with decreasing temperature.

For the lowest frequency phonon branch, the presence of electrons has virtually no effect on the dependence $\omega(q)$. For the branch with the next highest energy, the change in the optical phonon energy due to the presence of electrons in the QW does not exceed 0.6 meV . With increasing wave vector, the influence of electrons on the spectrum of optical phonons weakens and at $q > 1 \text{ nm}^{-1}$ it becomes negligible. The reason for this is the spatial dispersion of electronic polarizability, which leads to a decrease in the latter with increasing wave vector at fixed frequency. Figure 3 shows the spectra of odd phonons. Only the branch corresponding to bulklike phonons at (36 meV) is not shown, since it is practically not affected by the presence of electrons of the concentrations under consideration. From the comparison of Figs. 2 and 3

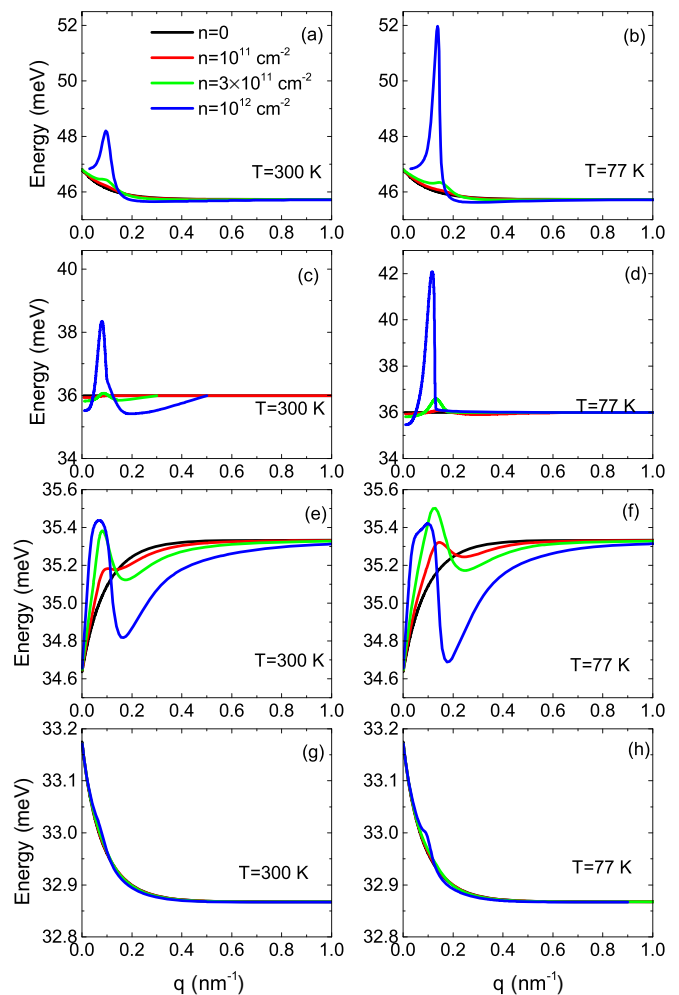


FIG. 2. Spectra of four branches of the even optical phonons calculated for four electron concentrations and two temperatures. Panels (c) and (d) correspond to the bulklike optical phonons.

it is clear that the influence of electrons in the QW on the spectrum of the odd optical phonons is noticeably weaker than on the spectrum of the even optical phonons. This is due to the well-known feature of plasma effects of two-dimensional electron gas, which are the physical cause of the influence of electrons on phonons. This feature, in particular, is manifested in the fact that the potential of two-dimensional plasmons is an even function of the coordinate normal to the plane of the quantum well, and odd two-dimensional plasmons do not exist [34].

Note that the presence of electrons in the quantum well leads to the existence of two more types of excitations, the spectra of which are not given in this work. One of them is a low-frequency plasmon, the frequency of which is proportional \sqrt{q} at small wave vectors. The second is an intersubband plasmon, the frequency of which is close to the energy difference between the first and second electron subbands. The probabilities of electron scattering by these excitations are small compared to the probabilities of scattering by the optical phonons. Therefore, these excitations are not considered in this work.

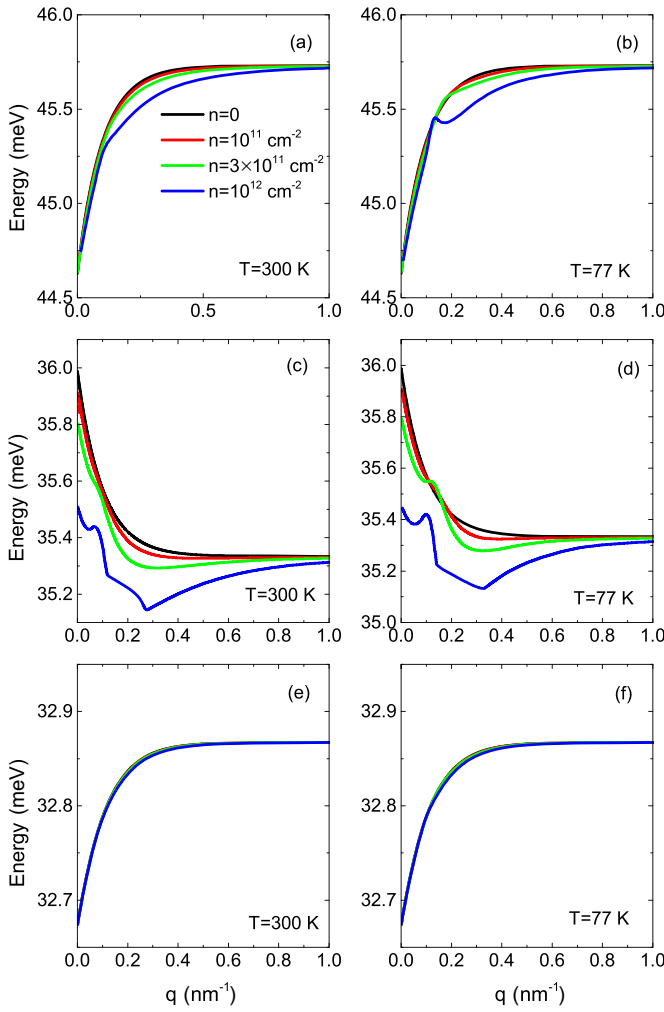


FIG. 3. Spectra of three branches of odd surface optical phonons calculated for four electron concentrations and two temperatures.

III. RATES OF ELECTRON-OPTICAL PHONON SCATTERING

A. Expressions for calculating scattering characteristics

It is well known that the main mechanism of scattering of Γ -valley electrons by optical phonons is the Frohlich mechanism [35]. In this mechanism, electrons interact with the macroscopic electric potential created by lattice vibrations [35]. The operator of the electric potential created by the optical phonon in the system under consideration can be represented as [22]

$$\hat{\varphi}_q^s(\mathbf{r}, t) = \Phi_{q,s}(z) \sqrt{\frac{\hbar\omega_{q,s}}{F_{q,s}(\omega_{q,s})}} [\hat{a}_{q,s} \exp(i\mathbf{q}\mathbf{r} - i\omega_{q,s}t) + \hat{a}_{q,s}^+ \exp(-i\mathbf{q}\mathbf{r} + i\omega_{q,s}t)], \quad (18)$$

where $\hat{a}_{q,s}^+$, $\hat{a}_{q,s}$ are the operators of creation and annihilation of the optical phonon with a wave vector \mathbf{q} and frequency $\omega_{q,s}$, and the subscript s denotes the type of optical phonon. The explicit form of the functions $F_{q,s}(\omega_{q,s})$ for even and odd phonons is given in Appendix C.

The probability of scattering of an electron with wave vector \mathbf{k} from the l th subband to the m th subband with the emission of the optical phonon has the form [35]

$$W_{\mathbf{k},l \rightarrow \mathbf{k}-\mathbf{q},m}^{+s} = \frac{2\pi}{\hbar} e^2 |\varphi_{\mathbf{k},l;\mathbf{k}-\mathbf{q},m}^s|^2 (N_q + 1) [1 - f_m(\mathbf{k} - \mathbf{q})] \times \delta[\varepsilon_l(\mathbf{k}) - \varepsilon_m(\mathbf{k} - \mathbf{q}) - \hbar\omega_{q,s}], \quad (19)$$

where $\varphi_{\mathbf{k},l;\mathbf{k}-\mathbf{q},m}^s$ is the matrix element of the electric potential operator and N_q is the number of phonons with wave vector q . Further we will assume that phonons are described by the Bose-Einstein distribution. The expression for the probability of scattering with phonon absorption has the form

$$W_{\mathbf{k},l \rightarrow \mathbf{k}+\mathbf{q},m}^{-s} = \frac{2\pi}{\hbar} e^2 |\varphi_{\mathbf{k},l;\mathbf{k}+\mathbf{q},m}^s|^2 N_q [1 - f_m(\mathbf{k} + \mathbf{q})] \times \delta[\varepsilon_l(\mathbf{k}) - \varepsilon_m(\mathbf{k} + \mathbf{q}) + \hbar\omega_{q,s}]. \quad (20)$$

Important scattering characteristics are the scattering frequency, the wave vector relaxation rate, and the electron energy relaxation rate [35]. The scattering frequency of an electron with wave vector k from the l th subband is equal to

$$W_l(k) = \sum_{\mathbf{q},s,m} (W_{\mathbf{k},l \rightarrow \mathbf{k}-\mathbf{q},m}^{+s} + W_{\mathbf{k},l \rightarrow \mathbf{k}+\mathbf{q},m}^{-s}) \quad (21)$$

The relaxation rate of the electron wave vector can be represented as

$$\mathbf{P}_l(\mathbf{k}) = \sum_{\mathbf{q},s,m} \mathbf{q} (W_{\mathbf{k},l \rightarrow \mathbf{k}-\mathbf{q},m}^{+s} - W_{\mathbf{k},l \rightarrow \mathbf{k}+\mathbf{q},m}^{-s}) \quad (22)$$

Due to the isotropy of the electron and phonon spectra in the plane of the quantum well, the vector $\mathbf{P}_l(\mathbf{k})$ is collinear with the wave vector \mathbf{q} .

The rate of electron energy relaxation due to scattering by optical phonons can be represented in the following form:

$$Q_l(k) = \sum_{\mathbf{q},s,m} \hbar\omega_{q,s} (W_{\mathbf{k},l \rightarrow \mathbf{k}-\mathbf{q},m}^{+s} - W_{\mathbf{k},l \rightarrow \mathbf{k}+\mathbf{q},m}^{-s}) \quad (23)$$

B. Intrasubband scattering

During intrasubband scattering, the parity of the electron wave function is preserved. Therefore, in symmetric wells, only even phonons can participate in intrasubband scattering. Calculations show that the main contribution to intrasubband scattering comes from scattering from a phonon mode, which is close in energy to the energy of a longitudinal optical phonon in GaAs (its contribution is $\sim 50\%$). The contribution of the lowest frequency surface mode to scattering is small ($\sim 1\%$). Figure 4 shows the dependencies of the scattering frequencies and the relaxation rate of the wave vector and energy on the initial wave vector of the electron for scattering in the first subband. From Fig. 4(a) it is clear that at $T = 300$ K in the range of wave vectors $0-0.4$ nm^{-1} the scattering frequency decreases with increasing electron concentration from 0 to 10^{11} cm^{-2} and from 3×10^{11} cm^{-2} to 10^{12} cm^{-2} . At $k > 0.4$ nm^{-1} , the dependence of the scattering frequency on the electron concentration is nonmonotonic. In this region, as the electron concentration increases to 3×10^{11} cm^{-2} , the scattering frequency decreases, and at a concentration of 10^{12} cm^{-2} , the scattering frequency increases significantly.

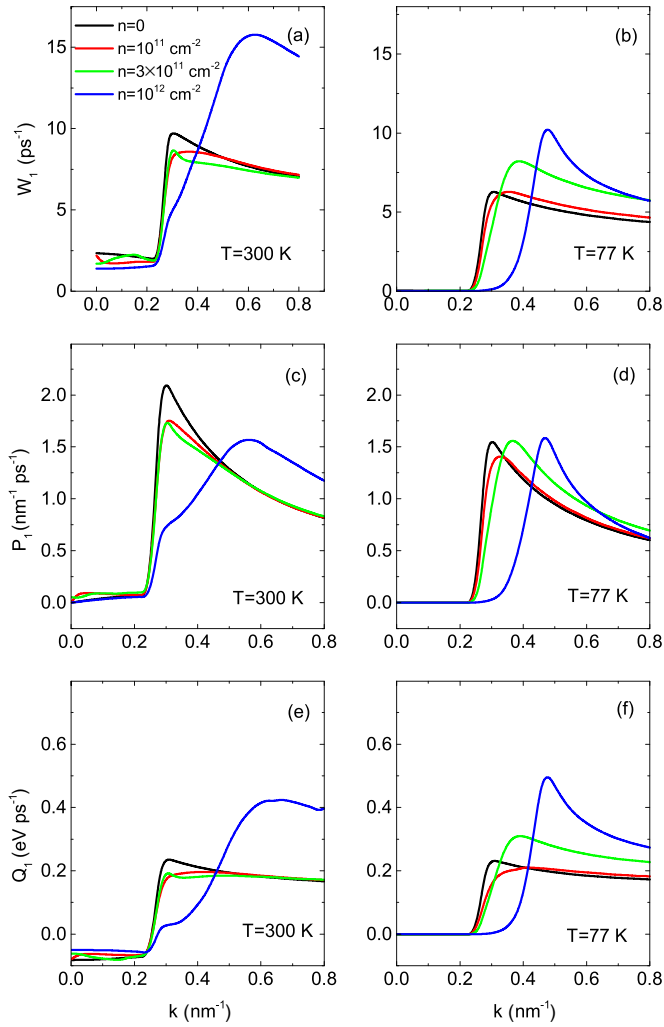


FIG. 4. Dependencies of the electron-optical phonon scattering frequency (a), (b), wave vector relaxation rate (c), (d), and energy relaxation rate (e), (f) on the initial electron wave number at $T = 300$ K and $T = 77$ K for four electron concentrations for scattering in the first subband.

A different situation occurs at $T = 77$ K. In this case, with increasing electron concentration, the scattering frequency increases, with the exception of those regions where scattering is affected by the electron filling of final states (the region to the left of the maximum scattering frequency). From the comparison of Figs. 4(a) and 4(b) it is clear that a decrease in temperature leads to a decrease in the scattering frequency, which is due to a decrease in the probability of scattering with the optical phonon absorption. The same reason leads to a decrease in the relaxation rate of the wave vector with decreasing temperature [see Figs. 4(c) and 4(d)].

From Figs. 4(c) and 4(d) it is clear that the maximum momentum relaxation rate monotonically decreases with increasing electron concentration at 300 K and changes slightly at 77 K. Note that at $T = 300$ K in the wave number range $0-0.4$ nm⁻¹ the momentum relaxation rate decreases with increasing electron concentration, similar to what occurs for the scattering frequency. A similar situation occurs for the absolute value of the energy relaxation rate at $T = 300$ K

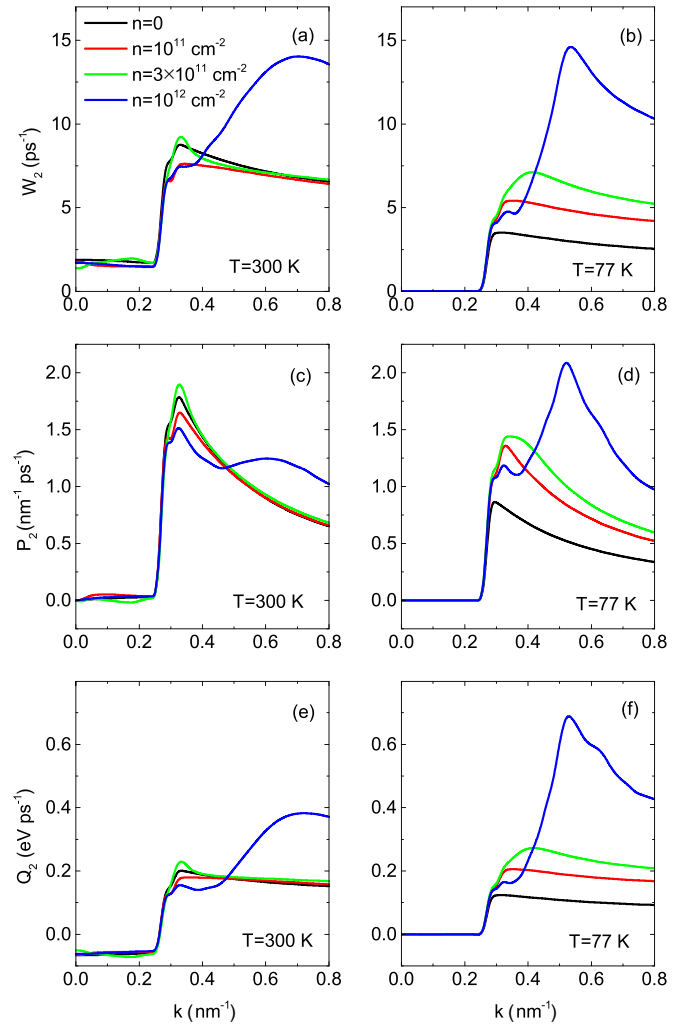


FIG. 5. Dependencies of the electron-optical phonon scattering frequency (a), (b), wave vector relaxation rate (c), (d), and energy relaxation rate (e), (f) on the initial electron wave number at $T = 300$ K and $T = 77$ K for four electron concentrations for scattering in the second subband.

[Fig. 4(e)], which in this wave number range decreases with increasing electron concentration. In the region of small wave numbers, this value is negative, which is due to the optical phonon absorption. At $T = 77$ K, the dependencies of the energy relaxation rate on the electron wave number and electron concentration are similar to corresponding dependencies for the scattering frequency.

Figure 5 shows the dependencies of the scattering frequency, wave vector relaxation rate, and energy on the initial electron wave number for the second electron subband. Due to the weak filling of the final electronic states, the wave vector from which scattering with phonon emission is “switched on” does not depend on the electron concentration. From the comparison of Figs. 4 and 5 it can be seen that the scattering frequencies and relaxation rates of the wave vector and energy are approximately the same for the first and second subbands. However, there is also a difference. In the second subband as the temperature decreases from 300 to 77 K, the scattering frequency for an electron concentration of 10^{12} cm⁻² changes slightly. In addition, the relaxation rates of the wave vector

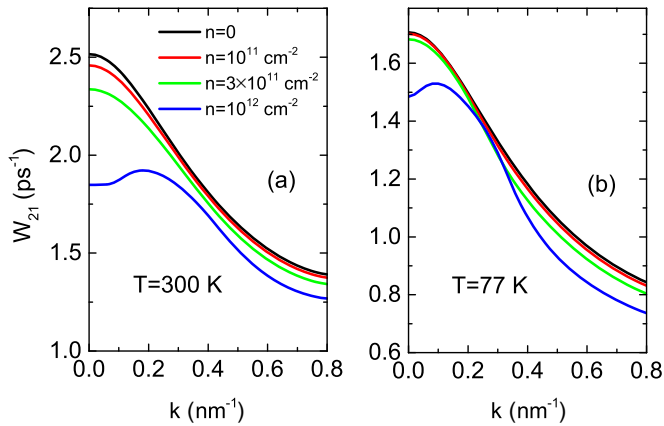


FIG. 6. Dependencies of the probability of intersubband scattering on the initial electron wave vector for two temperatures and four electron concentrations.

and energy for an electron concentration of 10^{12} cm^{-2} at 77 K in the second subband are significantly higher than in the first subband.

Note that the presence of electrons with the concentrations under consideration does not greatly change the phonon spectrum, but has a noticeable effect on the scattering frequencies and on the relaxation rates of the wave vector and energy. The reason for this is that the presence of electrons changes the potential created by the phonon. Therefore, the matrix element of the operator of electron-optical phonon interaction changes. Despite the small change in phonon energy, the change in the matrix element may not be small. For large phonon wave vectors, when electrons practically do not change the phonon energy, the matrix element of the electron-phonon interaction does not change. However, for small phonon wave vectors, the change in the matrix element of the electron-phonon interaction is not small. Note that as the electron wave vector increases, the minimum wave vector of the phonon, which can take part in scattering, decreases. In addition, the probability of scattering by polar phonons increases with decreasing phonon wave vector [35]. Therefore, the strongest effect on scattering can be seen for an electron concentration of 10^{12} cm^{-2} in the region of large initial electron wave vectors.

C. Intersubband scattering

Only odd optical phonons can take part in intersubband scattering, since such scattering changes the parity of the electron wave function. Figure 6 shows the dependence of the probability of electron scattering from the second subband into the first subband W_{21} on the initial electron wave vector for four electron concentrations and two temperatures. It can be seen from the figure that as the electron concentration increases, the probability of intersubband electron-optical phonon scattering decreases. This decrease is most clearly visible at a temperature of 300 K. However, in the range of electron concentrations considered, the decrease in probability is not large. The decrease in probability for small electron wave vectors at $n = 10^{12} \text{ cm}^{-2}$ is due to the Pauli principle, since a noticeable filling of the final electron states appears. From Fig. 6 it can be seen that with increasing temperature the

probability of intersubband scattering increases. The reason for this is the increase in the number of the optical phonons with increasing temperature.

Calculations show that the main contribution to intersubband electron scattering comes from a bulklike phonon mode with a phonon energy of about 36 meV, similar to intrasubband scattering. However, unlike intrasubband scattering, the probability of intersubband scattering on this mode is practically independent of the electron concentration. Therefore, the change in the probability of intersubband scattering with a change in the electron concentration occurs due to scattering on surface modes with energies of about 45 and 35 meV [Figs. 3(a) and 3(b)]. The surface mode with an energy of about 33 meV [Fig. 3(c)] makes a negligible contribution to the probability of intersubband electron scattering.

IV. CONCLUSION

In conclusion, we present the main results of the work and briefly discuss the some physical consequences of the influence of the electron concentration on the electron-optical scattering phonon. The main results of the work are as follows:

(i) The work proposes a scheme for calculating the influence of the concentration of free electrons in a quantum well on the spectrum of optical phonons and on electron-optical phonon scattering. Using the proposed scheme, the spectra of optical phonons in a 10-nm GaAs quantum well surrounded by $\text{Al}_{0.3}\text{Ga}_{0.7}\text{As}$ barriers were calculated. It is shown that the presence of free electrons has the greatest influence on the spectrum of two high-frequency optical phonons. This effect is strongest on phonons with a wave vector less than 1 nm^{-1} .

(ii) The influence of free electrons on intrasubband electron-optical phonon scattering in a 10-nm GaAs quantum well was studied. It is shown that the frequency of such scattering varies nonmonotonically with increasing electron concentration. The relaxation rates of the wave vector and energy for scattering in the first and second subbands of size quantization are found.

(iii) The influence of free electrons on the scattering of electrons from the second subband to the first with the participation of the optical phonons was studied. It is shown that with increasing electron concentration, the frequency of intersubband scattering decreases.

Let us now briefly discuss some physical consequences of the influence of electron concentration on electron-optical phonon scattering. From the presented results it is clear that the frequency of intrasubband electron-optical phonon scattering in GaAs is approximately an order of magnitude higher than the frequency of intersubband scattering. Therefore, in semiconductor laser diodes with GaAs quantum wells, a decrease in the probability of intersubband scattering with increasing concentration of nonequilibrium carriers accelerates the filling of the vicinity of the bottom of the second size quantization subband. This circumstance accelerates the switching of the laser radiation frequency from a value corresponding to the gap between the ground electron and hole subbands to a value corresponding to the gap between the excited subbands. This phenomenon is often observed in semiconductor laser diodes with increasing concentration of nonequilibrium carriers (see, for example, [36]).

In the case of QCLs, doping to create an electron concentration in the QW of up to 10^{12} cm^{-2} will lead to a decrease in intersubband scattering between subbands, electron transitions between which generate radiation. An increase in the time of electron scattering from the upper working subband to the lower one with the participation of optical phonons will lead to an increase in the difference in electron concentrations in these subbands and an increase in population inversion (see, for example, formula (1) in [37]). Therefore, QCLs with higher doping will have lower threshold current densities and higher maximum operating temperatures.

A decrease in the frequency of intersubband scattering with increasing electron concentration also improves the characteristics of quantum well photodetectors, since it prevents the return of a photoexcited electron from the second subband to the first one.

Data underlying the results presented in this paper are not publicly available at this time but may be obtained from the authors upon reasonable request.

ACKNOWLEDGMENT

The work was supported by the Russian Science Foundation (Project No. 23-19-00436).

APPENDIX A

In order to express Eq. (3) in the form of a one-dimensional integral, we use the method of obtaining electronic polarizability at any temperature from the expression for it at zero temperature [38]. An expression for electronic polarizability at zero temperature was obtained by Stern [34]. The essence of the method is as follows. Let us consider the difference between two polarizabilities $\chi(q, \omega, F)$, one of which corresponds to the chemical potential F , and the other to $F + \delta$. Then their difference corresponds to the contribution to the polarizability of filled electronic states located in the energy range from F to $F + \delta$. If δ is an infinitesimal value then this difference can be represented as

$$\chi(q, \omega, F + \delta) - \chi(q, \omega, F) = \delta \frac{\partial \chi(q, \omega, F)}{\partial F}. \quad (\text{A1})$$

In order to find the contribution of electronic states to polarizability in the range F to $F + \delta$ at nonzero temperature, it is necessary to multiply (A1) by the electron distribution function. Therefore, electronic polarizability at a finite temperature can be written as

$$\chi_T(q, \omega, F) = \int_0^\infty d\varepsilon \frac{\partial \chi(q, \omega, \varepsilon)}{\partial \varepsilon} \left[1 + \exp\left(\frac{\varepsilon - F}{k_B T}\right) \right]^{-1}, \quad (\text{A2})$$

where k_B is Boltzmann's constant. Integrating (A2) by parts we obtain the following expression for electronic polarizability:

$$\chi_T(q, \omega, F) = \frac{1}{4k_B T} \int_0^\infty d\varepsilon \chi(q, \omega, \varepsilon) \cosh^{-2}\left(\frac{\varepsilon - F}{2k_B T}\right). \quad (\text{A3})$$

Taking into account that $\kappa_{xx}^{\text{intra}}(q, \omega) = 4\pi d^{-1} \chi_T(q, \omega, F)$ and the explicit form of the real part $\chi(q, \omega, F)$ [34], we obtain the following expression for $\kappa_{xx}^{\text{intra}}(q, \omega)$:

$$\begin{aligned} \kappa_{xx}^{\text{intra}}(q, \omega) &= \frac{m_e e^2}{2\hbar^3 q^4 d k_B T} \int_0^\infty d\varepsilon \{2\hbar q^2 - c_- \theta_-(\varepsilon) \\ &\quad \times \sqrt{(\hbar q^2 - 2m_e \omega)^2 - 8m_e q^2 \varepsilon} \\ &\quad - \theta_+(\varepsilon) \sqrt{(\hbar q^2 + 2m_e \omega)^2 - 8m_e q^2 \varepsilon}\} \\ &\quad \times \cosh^{-2}\left(\frac{\varepsilon - F}{2k_B T}\right), \end{aligned} \quad (\text{A4})$$

where m_e is the effective electron mass,

$$c_- = \text{sgn}(\hbar q^2 - 2m_e \omega), \quad \text{sgn}(x) = x/|x|,$$

$\theta_\pm(\varepsilon) = \theta[(\hbar q^2 \pm 2m_e \omega)^2 - 8m_e q^2 \varepsilon]$, and $\theta(x)$ is the Heaviside function.

APPENDIX B

Let us consider the propagation along the QW of a wave that has a field component normal to the QW plane (z component) equal to $-E$. Let us consider the effect of this electric field component on the electron gas. This field component creates an electric potential:

$$\varphi(\mathbf{r}, t) = Ez(e^{i\mathbf{q}\mathbf{r} - i\omega t + \alpha t} + e^{-i\mathbf{q}\mathbf{r} + i\omega t + \alpha t}). \quad (\text{B1})$$

Using first order perturbation theory to find the wave functions $\psi(\mathbf{k}, \mathbf{r})$ and the definition for the z component of polarization:

$$\Pi_z(\mathbf{r}, t) = e \sum_{\mathbf{k}, l} f_l(\mathbf{k}) \int dz \psi_l^+(\mathbf{k}, \mathbf{r})_z \psi(\mathbf{k}, \mathbf{r}), \quad (\text{B2})$$

we find the following expression for it:

$$\begin{aligned} \Pi_z(\mathbf{r}, t) &= \frac{e^2 E}{S} (e^{i\mathbf{q}\mathbf{r} - i\omega t + \alpha t} + e^{-i\mathbf{q}\mathbf{r} + i\omega t + \alpha t}) \\ &\quad \times \sum_{\mathbf{k}, l, m} \left(\frac{|z_{\mathbf{k}+\mathbf{q}, m; \mathbf{k}, l}|^2}{\varepsilon_l(\mathbf{k}) - \varepsilon_m(\mathbf{k} + \mathbf{q}) + \hbar\omega + i\hbar\alpha} \right. \\ &\quad \left. + \frac{|z_{\mathbf{k}-\mathbf{q}, m; \mathbf{k}, l}|^2}{\varepsilon_l(\mathbf{k}) - \varepsilon_m(\mathbf{k} - \mathbf{q}) - \hbar\omega - i\hbar\alpha} \right). \end{aligned} \quad (\text{B3})$$

From Eq. (B3) it is clear that the polarization can be divided into two parts, proportional to $\exp(i\mathbf{q}\mathbf{r} - i\omega t + \alpha t)$ and $\exp(-i\mathbf{q}\mathbf{r} + i\omega t + \alpha t)$. Therefore, these parts can be considered separately.

Since $\Pi_z(\mathbf{r}, t) = -\chi E$ [the z component of the field is equal to $-E$ as it follows from (B1)], where χ is the polarizability of a unit volume, and the electron contribution to the dielectric permittivity can be written in the form $\kappa_{zz} = 4\pi \chi$, we find

$$\begin{aligned} \kappa_{zz}(q, \omega) &= \frac{4\pi e^2}{dS} \sum_{\mathbf{k}, l, m} \left(\frac{-|z_{\mathbf{k}+\mathbf{q}, m; \mathbf{k}, l}|^2}{\varepsilon_l(\mathbf{k}) - \varepsilon_m(\mathbf{k} + \mathbf{q}) + \hbar\omega + i\hbar\alpha} \right. \\ &\quad \left. + \frac{|z_{\mathbf{k}-\mathbf{q}, m; \mathbf{k}, l}|^2}{\varepsilon_l(\mathbf{k}) - \varepsilon_m(\mathbf{k} - \mathbf{q}) - \hbar\omega - i\hbar\alpha} \right) f_l(\mathbf{k}). \end{aligned} \quad (\text{B4})$$

If we make the following substitutions in the second term: $\mathbf{k} - \mathbf{q} \rightarrow \mathbf{k}$, $l \rightarrow m$, $m \rightarrow l$, then from Eq. (B4) we obtain Eq. (4). When $q \rightarrow 0$ from Eq. (B4) we obtain the formula for the contribution of intersubband transitions to the dielectric constant without taking into account spatial dispersion:

$$\kappa_{zz}(\omega) = -\frac{4\pi e^2}{dS} \sum_{\mathbf{k}, l, m} |z_{\mathbf{k}, l; \mathbf{k}, m}|^2 \frac{f_l(\mathbf{k}) - f_m(\mathbf{k})}{\varepsilon_l(\mathbf{k}) - \varepsilon_m(\mathbf{k}) - \hbar\omega}. \quad (\text{B5})$$

If we assume that the matrix element z does not depend on k , and the electron dispersion law is quadratic with the same mass in the subbands under consideration, then taking into account the contribution from only two subbands, (B4) can be represented as

$$\begin{aligned} \kappa_{zz}(q, \omega) = & \frac{4e^2 |z_{1,2}|^2}{d} \int dk \{ k f_1(k) [H(q, \omega, \Delta, k) \\ & + H(q, -\omega, \Delta, k)] + f_2(k) [H(q, \omega, -\Delta, k) \\ & + H(q, -\omega, -\Delta, k)] \}, \end{aligned} \quad (\text{B6})$$

where

$$H(q, \omega, \Delta, k) = \frac{\text{sgn}[G(q, \omega, \Delta)] \theta[G^2(q, \omega, \Delta) - b(k, q)]}{\sqrt{G^2(q, \omega, \Delta) - b(k, q)}}, \quad (\text{B7})$$

$$G(q, \omega, \Delta) = \Delta + \frac{\hbar^2 q^2}{2m_e} - \hbar\omega, \quad b(k, q) = \left(\frac{\hbar^2 k q}{m_e} \right)^2, \quad (\text{B8})$$

$$\Delta = \varepsilon_2(k) - \varepsilon_1(k).$$

APPENDIX C

Functions $F_{q,s}(\omega_{q,s})$ for even phonons were found in Ref. [22], but the functions in Ref. [22] were chosen differently from those in this paper. The functions $F_{q,s}(\omega_{q,s})$ are found from the following equation:

$$\begin{aligned} F_{q,s}(\omega_{q,s}) = & \frac{S}{2\pi} \left\{ \frac{\partial[\omega_{q,s}\kappa_{xx}(\omega_{q,s})]}{\partial\omega_{q,s}} \int_{-d/2}^0 dz q^2 \Phi_{q,s}^2(z) \right. \\ & + \frac{\partial[\omega_{q,s}\kappa_b(\omega_{q,s})]}{\partial\omega_{q,s}} \int_{-\infty}^{-d/2} dz \left[\Phi_{q,s}^2(z) + \left(\frac{\partial\Phi_{q,s}}{\partial z} \right)^2 \right] \\ & \left. + \frac{\partial[\omega_{q,s}\kappa_{zz}(\omega_{q,s})]}{\partial\omega_{q,s}} \int_{-d/2}^0 dz \left(\frac{\partial\Phi_{q,s}(z)}{\partial z} \right)^2 \right\}, \end{aligned} \quad (\text{C1})$$

where the right-hand side (C1) is the expression for the phonon energy, and the index s in $\Phi_{q,s}(z)$ denotes the branch of the phonon mode.

For bulklike even phonons this function has the form

$$\begin{aligned} F_{q,s} = & \frac{Sq}{8\pi} \left\{ \frac{4\partial[\omega_{q,s}\kappa_b(\omega_{q,s})]}{\partial\omega_{q,s}} \cos^2(\beta_q qd/2) \right. \\ & + \frac{\partial[\omega_{q,s}\kappa_{xx}(\omega_{q,s})]}{\partial\omega_{q,s}} \frac{[\beta_q qd + \sin(\beta_q qd)]}{\beta_q} \\ & \left. + \frac{\partial[\omega_{q,s}\kappa_{zz}(\omega_{q,s})]}{\partial\omega_{q,s}} \beta_q [\beta_q qd - \sin(\beta_q qd)] \right\}, \end{aligned} \quad (\text{C2})$$

where $\beta_q = \beta_q(\omega_{q,s})$

For surface even phonons this function has the form

$$\begin{aligned} F_{q,s} = & \frac{Sq}{8\pi} \left\{ \frac{4\partial[\omega_{q,s}\kappa_b(\omega_{q,s})]}{\partial\omega_{q,s}} \cosh^2(\gamma_q qd/2) \right. \\ & + \frac{\partial[\omega_{q,s}\kappa_{xx}(\omega_{q,s})]}{\partial\omega_{q,s}} \frac{[\gamma_q qd + \sinh(\gamma_q qd)]}{\beta_q} \\ & \left. + \frac{\partial[\omega_{q,s}\kappa_{zz}(\omega_{q,s})]}{\partial\omega_{q,s}} \gamma_q [-\gamma_q qd + \sinh(\gamma_q qd)] \right\}, \end{aligned} \quad (\text{C3})$$

where $\gamma_q = \gamma_q(\omega_{q,s})$.

For bulklike odd phonons this function has the form

$$\begin{aligned} F_{q,s} = & \frac{Sq}{8\pi} \left\{ \frac{4\partial[\omega_{q,s}\kappa_b(\omega_{q,s})]}{\partial\omega_{q,s}} \cos^2(\beta_q qd/2) \right. \\ & + \frac{\partial[\omega_{q,s}\kappa_{xx}(\omega_{q,s})]}{\partial\omega_{q,s}} \frac{[\beta_q qd - \sin(\beta_q qd)]}{\beta_q} \\ & \left. + \frac{\partial[\omega_{q,s}\kappa_{zz}(\omega_{q,s})]}{\partial\omega_{q,s}} \beta_q [\beta_q qd + \sin(\beta_q qd)] \right\}. \end{aligned} \quad (\text{C4})$$

For surface odd phonons this function has the form

$$\begin{aligned} F_{q,s} = & \frac{Sq}{8\pi} \left\{ \frac{4\partial[\omega_{q,s}\kappa_b(\omega_{q,s})]}{\partial\omega_{q,s}} \cosh^2(\gamma_q qd/2) \right. \\ & + \frac{\partial[\omega_{q,s}\kappa_{xx}(\omega_{q,s})]}{\partial\omega_{q,s}} \frac{[-\gamma_q qd + \sinh(\gamma_q qd)]}{\beta_q} \\ & \left. + \frac{\partial[\omega_{q,s}\kappa_{zz}(\omega_{q,s})]}{\partial\omega_{q,s}} \gamma_q [\gamma_q qd + \sinh(\gamma_q qd)] \right\}. \end{aligned} \quad (\text{C5})$$

-
- [1] M. Yoshida, S. Katsuno, T. Inoue, J. Gellela, K. Izumi, M. De Zoysa, K. Ishizaki, and S. Noda, High-brightness scalable continuous-wave single-mode photonic-crystal laser, *Nature (London)* **618**, 727 (2023).
- [2] L. Gao, C. Feng, and X. Zhao, Recent developments in terahertz quantum cascade lasers for practical applications, *Nanotechnol. Rev.* **12**, 20230115 (2023).
- [3] L. Shvartsman and B. Laikhtman, Fundamental limitations on gain of terahertz quantum cascade lasers, *J. Appl. Phys.* **134**, 063101 (2023).
- [4] B. Levine, Quantum-well infrared photodetectors, *J. Appl. Phys.* **74**, R1 (1993).
- [5] F. Fuchs and K. L. Kliewer, Optical modes of vibration in an ionic crystal slab, *Phys. Rev.* **140**, A2076 (1965).
- [6] K. Huang and B. Zhu, Dielectric continuum model and frohlich interaction in superlattices, *Phys. Rev. B* **38**, 13377 (1988).
- [7] B. C. Lee, K. W. Kim, M. A. Stroschio, and M. Dutta, Optical-phonon confinement and scattering in wurtzite heterostructures, *Phys. Rev. B* **58**, 4860 (1998).
- [8] S. M. Komirenko, K. W. Kim, M. A. Stroschio, and M. Dutta, Energy-dependent electron scattering via interaction with optical phonons in wurtzite crystals and quantum wells, *Phys. Rev. B* **61**, 2034 (2000).

- [9] E. P. Pokatilov and S. I. Beril, Electron-phonon interaction in periodic two-layer structures, *Phys. Status Solidi B* **118**, 567 (1983).
- [10] J. K. Jain and S. Das Sarma, Role of discrete slab phonons in carrier relaxation in semiconductor quantum wells, *Phys. Rev. Lett.* **62**, 2305 (1989).
- [11] N. Mori and T. Ando, Electron-optical-phonon interaction in single and double heterostructures, *Phys. Rev. B* **40**, 6175 (1989).
- [12] H. Rucker, E. Molinari, and P. Lugli, Electron-phonon interaction in quasi-two-dimensional systems, *Phys. Rev. B* **44**, 3463 (1991).
- [13] H. Rucker, E. Molinari, and P. Lugli, Microscopic calculation of the electron-phonon interaction in quantum wells, *Phys. Rev. B* **45**, 6747 (1992).
- [14] I. Lee, S. M. Goodnick, M. Gulia, E. Molinari, and P. Lugli, Microscopic calculation of the electron-optical-phonon interaction in ultrathin GaAs/Al_xGa_{1-x}As alloy quantum-well systems, *Phys. Rev. B* **51**, 7046 (1995).
- [15] R. Zheng and M. Matsuura, Electron-optical-phonon interaction in quantum wells consisting of mixed crystals, *Phys. Rev. B* **60**, 4937 (1999).
- [16] J. Požela, A. Namajunas, K. Pozela, and V. Juciene, Electrons and phonons in quantum wells, *Semiconductors* **33**, 956 (1999).
- [17] F. Macheda, T. Sohler, P. Barone, and F. Mauri, Electron-phonon interaction and phonon frequencies in two-dimensional doped semiconductors, *Phys. Rev. B* **107**, 094308 (2023).
- [18] T. Sohler, M. Gibertini, and M. J. Verstraete, Remote free-carrier screening to boost the mobility of Frohlich-limited two-dimensional semiconductors, *Phys. Rev. Mater.* **5**, 024004 (2021).
- [19] Z. Chen, J. Sjakste, J. Dong, A. Taleb-Ibrahimi, J.-P. Rueff, A. Shukla, J. Peretti, E. Papalazarou, M. Marsi, and L. Perfetti, Ultrafast dynamics of hot carriers in a quasi-two-dimensional electron gas on InSe, *Proc. Natl. Acad. Sci. USA* **117**, 21962 (2020).
- [20] A. Hauber and S. Fahy, Scattering of carriers by coupled plasmon-phonon modes in bulk polar semiconductors and polar semiconductor heterostructures, *Phys. Rev. B* **95**, 045210 (2017).
- [21] V. Y. Aleshkin and M. S. Zholudev, Optical phonons in quantum well with anisotropic permittivity, *Phys. E (Amsterdam, Neth.)* **157**, 115863 (2024).
- [22] V. Y. Aleshkin, O. L. Domnina, and M. S. Zholudev, Electron-optical phonon scattering in a quantum well of HgTe/CdHgTe heterostructure, *Phys. Rev. B* **109**, 075307 (2024).
- [23] A. A. Dubinov and V. Y. Aleshkin, Model of a terahertz quantum-cascade laser based on a two-dimensional plasmon, *Semiconductors* **55**, 828 (2021).
- [24] D. A. Dahl and L. J. Sham, Electrodynamics of quasi-two dimensional electrons, *Phys. Rev. B* **16**, 651 (1977).
- [25] C. J. van der Poel, H. P. M. M. Ambrosius, R. W. M. Linders, R. M. L. Peeters, G. A. Acket, and M. P. C. M. Krijn, Strained layer GaAs_{1-y}P_y-AlGaAs and In_xGa_{1-x}As-AlGaAs quantum well diode lasers, *Appl. Phys. Lett.* **63**, 2312 (1993).
- [26] T. R. Tolliver, N. G. Anderson, F. Agahi, and K. M. Lau, Characteristic temperature study of GaAsP-AlGaAs tensile strained quantum well lasers, *J. Appl. Phys.* **88**, 5400 (2000).
- [27] A. Y. Andreev, A. Y. Leshko, A. Lyutetskii, A. Marmalyuk, T. Nalyot, A. Padalitsa, N. A. Pikhtin, D. Sabitov, V. Simakov, S. Slipchenko, M. Khomylev, and I. Tarasov, High-power laser diodes ($\lambda = 808\text{--}850\text{ nm}$) based on asymmetric separate-confinement heterostructures, *Semiconductors* **40**, 611 (2006).
- [28] L. Bosco, M. Franckie, G. Scaliari, M. Beck, A. Wacker, and J. Faist, Thermoelectrically cooled THz quantum cascade laser operating up to 210 K, *Appl. Phys. Lett.* **115**, 010601 (2019).
- [29] A. Khalatpour, A. Paulsen, C. Deimert, Z. Wasilewski, and Q. Hu, High-power portable terahertz laser systems, *Nat. Photonics* **15**, 16 (2021).
- [30] A. Khalatpour, M. C. Tam, S. J. Addamane, J. Reno, Z. Wasilewski, and Q. Hu, Enhanced operating temperature in terahertz quantum cascade lasers based on direct phonon depopulation, *Appl. Phys. Lett.* **122**, 161101 (2023).
- [31] V. Y. Aleshkin and A. A. Dubinov, Effect of the spin-orbit interaction on intersubband electron transition in GaAs/AlGaAs quantum well heterostructures, *Phys. B: Condens. Matter* **503**, 32 (2016).
- [32] J. S. Blakemore, Semiconducting and other major properties of gallium arsenide, *J. Appl. Phys.* **53**, R123 (1982).
- [33] D. J. Lockwood and Z. R. Wasilewski, Optical phonons in Al_xGa_{1-x}As: Raman spectroscopy, *Phys. Rev. B* **70**, 155202 (2004).
- [34] F. Stern, Polarizability of a two-dimensional electron gas, *Phys. Rev. Lett.* **18**, 546 (1967).
- [35] V. F. Gantmakher and I. B. Levinson, *Carrier Scattering in Metals and Semiconductors* (North-Holland, Amsterdam, 1987).
- [36] M. Mittelstein, Y. Arakawa, A. Larsson, and A. Yariv, Second quantized state lasing of a current pumped single quantum well laser, *Appl. Phys. Lett.* **49**, 1689 (1986).
- [37] J. Faist, D. Hofstetter, M. Beck, T. Aellen, M. Rochat, and S. Blaser, Bound-to-continuum and two-phonon resonance, quantum-cascade lasers for high duty cycle, high-temperature operation, *IEEE J. Quantum Electron.* **38**, 533 (2002).
- [38] A. F. Page, J. M. Hamm, and O. Hess, Polarization and plasmons in hot photoexcited graphene, *Phys. Rev. B* **97**, 045428 (2018).